Optics Letters

Ultrabroadband tunable OPA design using a spectrally broadened pump source

Seyed Ali Rezvani,[1] Zuofei Hong,[2] Xiaoxiao Pang,[1] Shun Wu,[3,4] Qingbin Zhang,[1,*] and Peixiang Lu[1,2]

[1]Wuhan National Laboratory for Optoelectronics and School of Physics, Huazhong University of Science and Technology, Wuhan 430074, China
[2]Laboratory of Optical Information Technology, Wuhan Institute of Technology, Wuhan 430074, China
[3]Department of Physics, University of California, Berkeley, California 94720, USA
[4]e-mail: wushun@berkeley.edu
*Corresponding author: zhangqingbin@hust.edu.cn

Received 5 July 2017; revised 26 July 2017; accepted 27 July 2017; posted 28 July 2017 (Doc. ID 301700); published 23 August 2017

A robust optical parametric amplifier (OPA) scheme is proposed in which we have experimentally achieved broadband bandwidth for a collinear OPA design that exhibits good beam quality and spatial distribution using a type-I β barium borate crystal. The applied pump pulses are simultaneously spectrally broadened and temporally stretched in a multi-plate system before being used to amplify the temporally stretched white light. In this case, the phase matching can be obtained for a broad range of wavelengths, and we have managed to achieve bandwidths three times broader than a conventional narrowband pumped collinear OPA. With a bandwidth as broad as 400 nm centered at 1400 nm, as well as a broadband angular dispersion-free idler, the signal bandwidth supports transform-limited pulses as short as 7.5 fs which correspond to sub-two optical cycles for this center wavelength. Furthermore, the system is easily tunable over a 400 nm range of bandwidths starting from 1100 to 1500 nm. The proposed scheme provides a versatile near-infrared/middle-infrared source with a broad bandwidth and fine tuning capability which paves the way for ultrafast spectroscopy and strong field applications.

OCIS codes: (140.3070) Infrared and far-infrared lasers; (190.4970) Parametric oscillators and amplifiers; (190.2620) Harmonic generation and mixing.

https://doi.org/10.1364/OL.42.003367

The few-cycle pulses have been recognized as one of the most useful tools for revealing and manipulating ultrafast electron dynamics within the attosecond timescale, which opens the doors to the attosecond science [1,2]. With the rapid advancement of few-cycle laser technology operated around 800 nm using the Ti:sapphire medium, so far the shortest isolated attosecond pulses attained have been pushed forward to an unprecedented sub-100 attoseconds region [3,4].

However, it was soon realized that the invariable center wavelength of the few-cycle pulse becomes the bottleneck for the further development of its applications. Few-cycle pulses with longer wavelengths are promising sources for scaling attosecond pulses toward higher photon energies and shorter pulse durations [5–7]. Middle-infrared (MIR) few-cycle pulses also can be used for achieving fine manipulation of electron dynamics individually, or they can be effective when accompanied by the fundamental laser in tailoring the driver field and giving it the additional capacity of being tunable [8,9]. Moreover, few-cycle pulses provide the opportunity of broadband vibrational spectroscopy, time-resolved optical spectroscopy, and many other precise measurement techniques. Therefore, advancements in the generation of few-cycle pulses have remarkable contributions to the ultrafast spectroscopy and, consequently, the generation of broadband ultrashort pulses at longer wavelengths as a straightforward approach is highly desirable.

An ideal IR pulse to this end is required to have the following properties: (1) ultrabroad bandwidth for supporting extreme short pulse duration, (2) superior tunability, (3) good spatial quality, and (4) scalable energy. Even though achieving any of these characteristics is nontrivial in general, optical parametric amplification (OPA) has been proven to be the most efficient scheme to perform this task [10–12]. The most critical limiting factor that restrains OPA systems from achieving ultrabroadband gains is the phase mismatch. The first order phase mismatch is, in fact, the group velocity mismatch between the interacting waves that yields the highest impact on the OPA limitations. In order to negate this limitation, operating OPA systems at degeneracy has been proposed; examples of such systems can be found in [13–17]. This solution comes with the limitation on the tunability. Alternatively, noncollinear OPA (NOPA) schemes have been introduced [18]. In NOPA, the interaction angles are chosen so that the signal group velocity is equal to the projection of the idler group velocity along the signal's direction. Many different NOPA schemes have been recommended [19–22]. NOPA systems are capable of providing tunable broad bandwidths required for few-cycle pulse generation; however, the idler generated in NOPA suffers from the angular dispersion. This dispersion is caused by the introduced noncollinear angle, and it requires energy consuming compensation methods or signal wavefront manipulation to be removed [23]. Since NOPA requires idler group velocity to be greater than the signal's, it can only be applied using specific

nonlinear crystals and a type of phase-matching geometry. It has been demonstrated by Brida *et al.* that NOPA systems are capable of generating near-infrared pulses with two-cycle transform-limited (TL) duration, exploiting the high refractive index of a periodically poled stoichiometric lithium tantalate (PPLST) crystal [24]. Schmidt *et al.* managed to achieve broadband NOPA using type-II geometry in a barium borate (BBO) crystal [25]. Further studies in NOPA have shown that, in order to obtain maximum gain bandwidth, two signal wavelength components at different sides of central wavelength are chosen to be perfectly phase matched with the pump, and this results in a non-Gaussian amplified spectrum [26]. In order to overcome the inherited phase-matching limitation imposed by a specific cutting angle of the nonlinear crystal, Schmidt *et al.* introduced frequency domain OPA, where different frequencies of a broadband seed will be amplified independently in a parametric process using different BBO crystals with different cutting angles [27].

In this Letter, we introduce a collinear spectrally broadband pumped OPA scheme in which different pump and signal component pairs are phase matched in different time slices in a single crystal, and an ultrabroadband amplified signal is achieved that can be a perfect seeding source for high-energy applications. The search for power scalable systems that can achieve high-energy pulses in MIR and IR regions has been escalated by the prospect of using high harmonics to achieve table–top water window *x*-ray sources [28]. Optical parametric chirped pulse amplification (OPCPA), which considers temporally stretching pump or seed or both to achieve a better overlap and, therefore, higher efficiency, has been introduced and has shown great capabilities [29–31]. The application of the chirp-compensation scheme was experimentally investigated by Tang *et al.* in order to extend the gain bandwidth of OPCPA systems using a relatively narrowband 400 nm pump [32]. Following their footsteps, Zeng *et al.* have done a detailed theoretical study on optimized chirp-compensation schemes, and it has been illustrated that for specific pump-seed chirp ratios the gain narrowing effect can be overturned, and optimized gain bandwidths can be obtained [33]. A recent theoretical study by Yin *et al.* has shown that using this concept broadband Ti:sapphire pump pulses can be very well phased matched in a temporal domain [34] and have the potential to generate 3.2 μm few-cycle pulses in an OPA using a MgO:$LiNbO_3$ crystal. Our design experimentally introduces a compact system in which ultrabroadband MIR pulses are achieved exploiting the chirp matching of a spectrally broadband pump and seed. The proposed broadband pumped OPA design manipulates the temporal and spectral characteristics of the pump pulses simultaneously. This task is carried out by generating the broadband pump pulses using a recently developed multi-plate design made of fused silica [35–37]. The narrowband pump pulses (NBPs) from a commercially available 1 kHz, 35 fs Ti-sapphire source centered at 800 nm travel through four thin fused silica plates with the thickness of 100 μm and are spectrally broadened to a three times wider bandwidth, while they are being temporally stretched. Figure 1(a) depicts the schematic design of the system.

The NBP is focused into the fused silica plates by a convex lens which makes the intensity high enough to trigger self-phase modulation. New components near the center wavelength start to appear. An NBP enters the plates in angles close to the Brewster angle. The angles have been set to the Brewster angle at first and then slightly changed to achieve the largest bandwidth. The output broadband pump pulses have 210 μJ energy. The bandwidth broadening continues until the fourth plate, after which the bandwidth reaches 73 nm extents; that is 2.7 times broader than the initial bandwidth (27 nm). The spectrum of the narrowband pump before the plates and after broadening is shown in Fig. 1(b). Broadband pump (BBP) pulse duration has been measured by second-harmonic-generation frequency-resolved optical gating (SHG-FROG), and it has been observed that pump pulses after broadening have 87 fs duration while they contain close to linear chirp. The results are shown in Fig. 2. The increased pulse duration in our system can increase the splitting length of the interacting waves [13] but, at the same time, the system benefits from a better overlap for the components covered under pump peak intensity, which has been shown to improve the bandwidth of an OPA system [38].

The broadband pump will be combined with the white light, generated in a white light generation system, in a dichroic mirror, and the combination will be loosely focused into a 2.4 mm type-I BBO cut at $\theta = 20°$. It has been closely controlled that the two beams enter the nonlinear crystal in a collinear manner only a small noncollinear angle $\phi \ll 1°$ has been

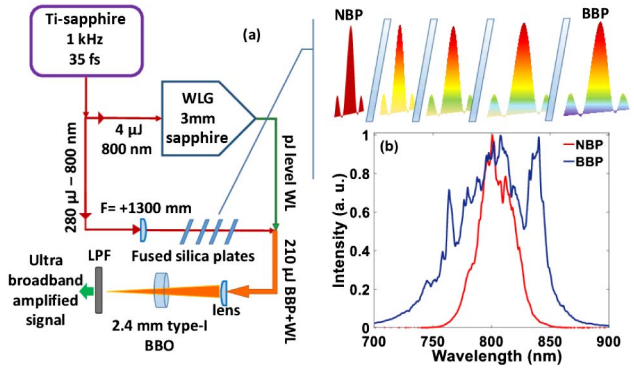

Fig. 1. (a) Schematic of the broadband OPA system. (b) Spectrum of a narrowband pump and the broadband pump generated in a multi-plate system. LPF, long-pass filter.

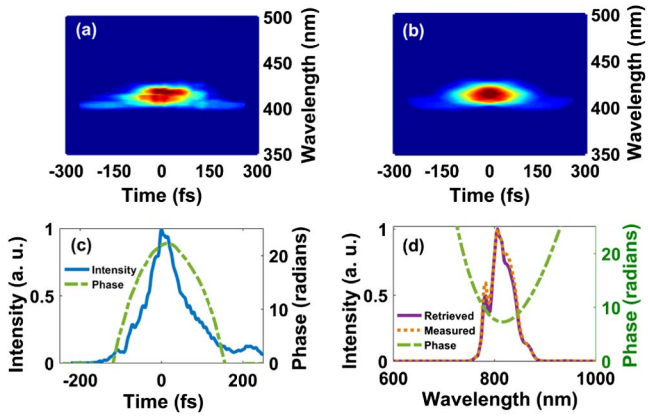

Fig. 2. (a) Experimental SHG-FROG trace, (b) retrieved SHG-FROG trace, (c) intensity and phase as a function of time, and (d) measured and retrieved spectral intensity and the retrieved phase.

introduced in order to separate the amplified signal and the idler for the later measurements.

The seed has been amplified once with the initial narrowband pump and once with the broadband pump in order to make an objective comparison between both cases. It has been observed that the amplified signal using BBP shows excellent bandwidth and beam quality. Figure 3(a) shows the bandwidth of both cases. NBP-OPA results in 141 nm bandwidth centered around 1400 nm, while having the same center wavelength the BBP-OPA scheme will result in a 400 nm bandwidth which is almost three times larger than the NBP-OPA. As we mentioned before, tunability of the center wavelength is an important property, for an OPA system. The proposed BBP-OPA has shown tunability over a wide range of wavelengths far from degeneracy, starting from 1100 to 1500 nm. Figure 3(b) presents the recorded spectrum for the amplified signal over three different center wavelengths in this range.

In order to explain the observed broad amplified signal's bandwidth of the BBP-OPA, we have numerically calculated phase-matching efficiency as a function of signal and pump wavelengths. This efficiency is defined as $\mathrm{Sinc}^2(\Delta kL/2)$, where Δk is the propagation constant difference, and L is the length of the BBO crystal. The results are shown in Fig. 4. As shown in the figure, phase matching for signal components covering

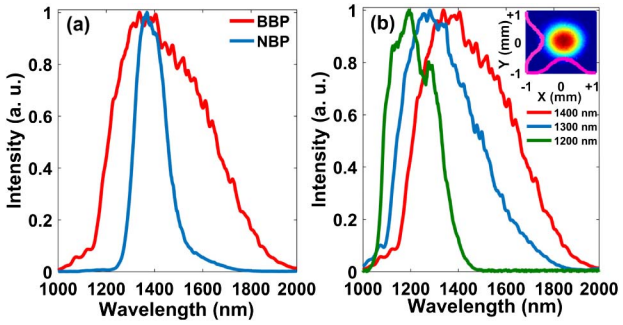

Fig. 3. (a) Spectrum of the amplified signal for NBP and BBP. (b) Spectrum of the amplified signal for different wavelengths over the tunability range. Inset: beam quality, measured using a 5 MP CCD camera.

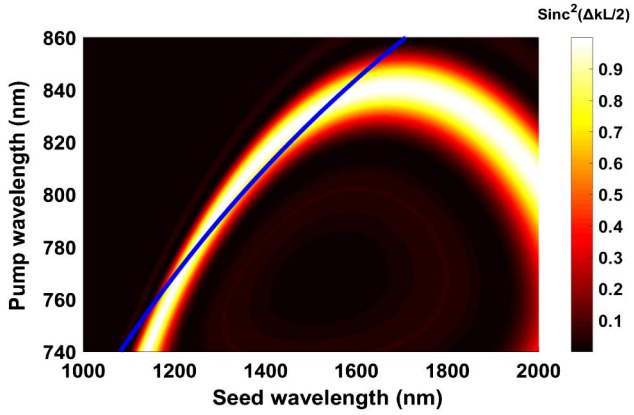

Fig. 4. Phase matching efficiency as a function of pump and seed spectrum for a BBO cut at $\theta = 20°$; the blue line denotes the linear chirp-compensation fitting.

1100–1700 nm can be achieved for pump components covering a 740–860 nm range. The simplest optimized seed to pump chirp relationship is the linear fit. Considering 800 pump and 1400 nm signal pulses, the slope of the linear fit, defined as $A = b_s/b_p$, where b_s and b_p are seed and pump chirps, accordingly, is $A = 1.8$. This linear fit is depicted on Fig. 4 by the blue line. Chirp of the pump and seed pulses can be calculated as $b_i = \zeta_i/(8\eta_i^2 + 2\zeta_i^2)$, where $i = p, s$ represents pump and seed, accordingly, and ζ_i is the group delay dispersion (GDD), $\eta_i = 2ln2/D_{\omega i}^2$ and $D_{\omega i}$ denotes the full width at half-maximum (FWHM) of the pulses in the frequency domain under Gaussian assumption. The details on how this equation has been obtained can be found in [30]. In our system, the pump is centered at 800 nm with 450 fs^2 GDD, and the seed is centered at 1400 nm and 240 fs^2 GDD, calculating the chirps with these parameters; the obtained chirp ratio is therefore set at $A = 1.8$.

As presented in Fig. 1, the FWHM of pump pulses in our BBP-OPA system covers 770–850 nm components. For this bandwidth, the linear fit overlap with the phase-matching trend predicts that the efficient phase matching can be achieved for signal pulses starting from 1170 to 1660 nm, accordingly. This is in perfect accord with the FWHM bandwidth obtained experimentally by BBP-OPA and is presented in Fig. 3(a).

The recorded bandwidths over the tunability range are obtained by changing the BBO angle and the delay in order to change the center wavelength. The GDD of the pulses was kept fixed and invariable. These results are also in good accord with the predicted values extracted from the phase-matching efficiency plot for different center wavelengths. The efficient overlap between linear fit ($A = 1.8$) and the phase-matching efficiency trend predict the amplified signal bandwidth to cover 1240–1560 nm components for signal pulses centered at 1300 nm wavelength. This is compatible with the recorded spectrum covering 1140–1504 nm. For signal pulses centered at 1200 nm, the overlap between the linear fit and phase-matching efficiency trend predicts efficient amplification for a range covering 1183–1316 nm which is also very well matched with the recorded spectra covering 1068–1320 nm FWHM. The bandwidth in the narrowest cases is still twice the size of the NBP-OPA bandwidth. The inset of Fig. 3(b) depicts the beam quality of the amplified beam centered at 1400 nm. The beam profile has been recorded, while the beam has been slightly focused into a 5-megapixel charge-coupled device (CCD) camera. The beam quality shows very good properties; the intensity profile on both axes is depicted by the pink lines. This excellent beam quality makes it easy to add secondary stages and further amplify the beam, as one of the most important factors in OPA systems is the beam quality at the nonlinear crystal. Using identical pump energies (180 μJ at the BBO's aperture), both NBP and BBP OPAs have shown lower than 3% conversion efficiencies. The output pulses of the NBP-OPA have 5 μJ energy, while the output of the BBP design reaches 3 μJ. Energy stability of less than 1% RMS has been measured for a BBP-OPA's signal over 3 h. Although the output of the BBP design is slightly lower than the NBP scheme, but the generated signal and idler pulses in this stage can easily be further amplified in a noncollinear second stage separately or be used as a seed in a DC-OPA to reach desired energy values if necessary [39]. Also as shown in [37], multi-plate systems are not restricted to the applied pump

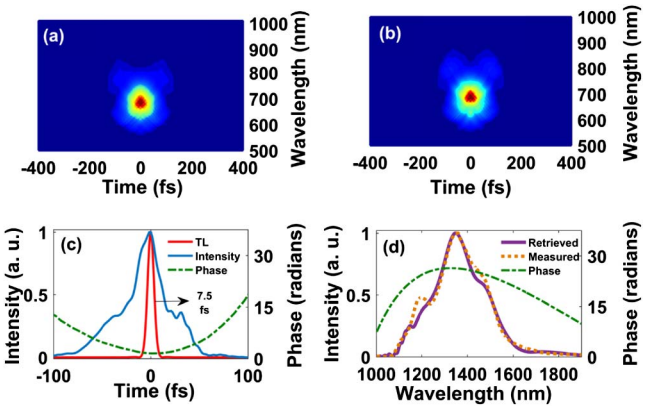

Fig. 5. (a) Experimental SHG-FROG trace. (b) Retrieved trace with 0.028 reconstruction error. (c) Temporal shape of the pulse retrieved from SHG-FROG (blue line), a 7.5 fs correspondent theoretical TL pulse (red line), and phase (green dashed line). (d) Measured and retrieved spectral intensity and the retrieved phase.

energy of our experiment, and higher pump powers can be used, which can improve the output power of the system.

Temporal properties of the amplified signal have been measured using SHG-FROG. The results are presented in Fig. 5. The uncompressed signal has 34 fs pulse duration. Theoretically, such pulse duration can be compressed to a near TL value using various designs such as an adaptive system of prisms or gratings combined with a deformable mirror [14,24,26,40], acousto-optic programmable dispersive filter accompanied by a bulk material [41], or using a customized chirp mirror set [40]. The theoretically calculated TL pulse for the amplified signal centered at 1400 nm with a 400 nm bandwidth, is depicted by the red line in Fig. 5.

In conclusion, we have proposed a MIR-OPA design that is pumped by a spectrally broadened source and is capable of obtaining an amplified signal bandwidth, three times wider than a conventionally narrowband pumped OPA system. The output shows good beam quality and temporal profile. The proposed design experimentally proves the positive impact of the broadband pump in OPA and can be used as an ideal pre-amplification stage for high-energy applications. The scheme is easily tunable over a 400 nm range and can be used in applications in which the center wavelength plays a key role.

Funding. National Natural Science Foundation of China (NSFC) (11574101, 11627809, 11234004).

REFERENCES

1. F. Krausz and M. Ivanov, Rev. Mod. Phys. **81**, 163 (2009).
2. E. Goulielmakis, Z. H. Loh, A. Wirth, R. Santra, N. Rohringer, V. S. Yakovlev, S. Zherebtsov, T. Pfeifer, A. M. Azzeer, M. F. Kling, S. R. Leone, and F. Krausz, Nature **466**, 739 (2010).
3. E. Goulielmakis, M. Schultze, M. Hofstetter, V. S. Yakovlev, J. Gagnon, M. Uiberacker, A. L. Aquila, E. M. Gullikson, D. T. Attwood, R. Kienberger, F. Krausz, and U. Kleineberg, Science **320**, 1614 (2008).
4. K. Zhao, Q. Zhang, M. Chini, Y. Wu, X. Wang, and Z. Chang, Opt. Lett. **37**, 3891 (2012).
5. N. Ishii, K. Kaneshima, K. Kitano, T. Kanai, S. Watanabe, and J. Itatani, Nat. Commun. **5**, 3331 (2014).
6. S. L. Cousin, F. Silva, S. Teichmann, M. Hemmer, B. Buades, and J. Biegert, Opt. Lett. **39**, 5383 (2014).
7. F. Silva, S. M. Teichmann, S. L. Cousin, M. Hemmer, and J. Biegert, Nat. Commun. **6**, 6611 (2015).
8. E. J. Takahashi, P. Lan, O. D. Mücke, Y. Nabekawa, and K. Midorikawa, Nat. Commun. **4**, 2691 (2013).
9. Q. Zhang, L. He, P. Lan, and P. Lu, Opt. Express **22**, 13213 (2014).
10. J. W. Yoon, S. K. Lee, T. J. Yu, J. H. Sung, T. M. Jeong, and J. Lee, Curr. Appl. Phys. **12**, 648 (2012).
11. H. Xiong, H. Xu, Y. Fu, J. Yao, B. Zeng, W. Chu, Y. Cheng, Z. Xu, E. J. Takahashi, K. Midorikawa, X. Liu, and J. Chen, Opt. Lett. **34**, 1747 (2009).
12. E. J. Takahashi, Y. Tamaru, Y. Fu, O. D. Müecke, F. X. Kaertner, A. Suda, and K. Midorikawa, *Conference on Lasers and Electro-Optics*, OSA Technical Digest (online) (Optical Society of America, 2016), paper FTh1M.6.
13. G. Cerullo and S. De Silvestri, Rev. Sci. Instrum. **74**, 1 (2003).
14. D. Brida, G. Cirmi, C. Manzoni, S. Bonora, P. Villoresi, S. De Silvestri, and G. Cerullo, Opt. Lett. **33**, 741 (2008).
15. S. Hädrich, J. Rothhardt, F. Röser, T. Gottschall, J. Limpert, and A. Tünnermann, Opt. Express **16**, 19812 (2008).
16. J. Limpert, C. Aguergaray, S. Montant, I. Manek-Hönninger, S. Petit, D. Descamps, E. Cormier, and F. Salin, Opt. Express **13**, 7386 (2005).
17. A. M. Siddiqui, G. Cirmi, D. Brida, F. X. Kärtner, and G. Cerullo, Opt. Lett. **34**, 3592 (2009).
18. T. Wilhelm, J. Piel, and E. Riedle, Opt. Lett. **22**, 1494 (1997).
19. J. Zheng and H. Zacharias, Appl. Phys. B **97**, 765 (2009).
20. T. J. Wang, Z. Major, I. Ahmad, S. A. Trushin, F. Krausz, and S. Karsch, Appl. Phys. B **100**, 207 (2010).
21. O. Isaienko and E. Borguet, J. Opt. Soc. Am. B **26**, 965 (2009).
22. A. Shirakawa, I. Sakane, M. Takasaka, and T. Kobayashi, Appl. Phys. Lett. **74**, 2268 (1999).
23. S. Huang, J. Moses, and F. X. Kärtner, Opt. Lett. **37**, 2796 (2012).
24. D. Brida, S. Bonora, C. Manzoni, M. Marangoni, P. Villoresi, S. De Silvestri, and G. Cerullo, Opt. Express **17**, 12510 (2009).
25. C. Schmidt, J. Bühler, A. Heinrich, A. Leitenstorfer, and D. Brida, J. Opt. **17**, 094003 (2015).
26. G. Cirmi, D. Brida, C. Manzoni, M. Marangoni, S. De Silvestri, and G. Cerullo, Opt. Lett. **32**, 2396 (2007).
27. B. E. Schmidt, N. Thiré, M. Boivin, A. Laramée, F. Poitras, G. Lebrun, T. Ozaki, H. Ibrahim, and F. Légaré, Nat. Commun. **5**, 3643 (2014).
28. E. J. Takahashi, T. Kanai, K. L. Ishikawa, Y. Nabekawa, and K. Midorikawa, Phys. Rev. Lett. **101**, 253901 (2008).
29. Z. Hong, Q. Zhang, P. Lan, and P. Lu, Opt. Express **22**, 5544 (2014).
30. Q. Zhang, E. Takahashi, O. Mücke, P. Lu, and K. Midorikawa, Opt. Express **19**, 7190 (2011).
31. J. Rothhardt, S. Demmler, S. Hädrich, J. Limpert, and A. Tünnermann, Opt. Express **20**, 10870 (2012).
32. Y. Tang, I. N. Ross, C. Hernandez-Gomez, G. H. C. New, I. Musgrave, O. V. Chekhlov, P. Matousek, and J. L. Collier, Opt. Lett. **33**, 2386 (2008).
33. S. Zeng, B. Zhang, Y. Dan, X. Li, N. Sun, and Z. Sui, Opt. Commun. **283**, 4054 (2010).
34. Y. Yin, J. Li, X. Ren, Y. Wang, A. Chew, and Z. Chang, Opt. Express **24**, 24989 (2016).
35. Y. Cheng, C. H. Lu, Y. Lin, and A. H. Kung, Opt. Express **24**, 7224 (2016).
36. C. Lu, Y. Tsou, H. Chen, B. Chen, Y. Cheng, S. Yang, M. Chen, C. Hsu, and A. H. Kung, Optica **1**, 400 (2014).
37. P. He, Y. Liu, K. Zhao, H. Teng, X. He, P. Huang, H. Huang, S. Zhong, Y. Jiang, S. Fang, X. Hou, and Z. Wei, Opt. Lett. **42**, 474 (2017).
38. S. A. Rezvani, Q. Zhang, Z. Hong, and P. Lu, Opt. Express **24**, 11187 (2016).
39. Y. Fu, E. J. Takahashi, and K. Midorikawa, Opt. Lett. **40**, 5082 (2015).
40. D. Brida, C. Manzoni, G. Cirmi, M. Marangoni, S. Bonora, P. Villoresi, S. De. Silvestri, and G. Cerullo, J. Opt. **12**, 013001 (2009).
41. N. Ishii, K. Kaneshima, K. Kitano, T. Kanai, S. Watanabe, and J. Itatani, Opt. Lett. **37**, 4182 (2012).